Influence of chain topology and bond potential on the glass transition of polymer chains simulated with the bond fluctuation model

2008 J. Phys.: Condens. Matter 20 285102

(http://iopscience.iop.org/0953-8984/20/28/285102)

IOP Publishing Journal of Physics: Condensed Matter

J. Phys.: Condens. Matter **20** (2008) 285102 (10pp) doi:10.1088/0953-8984/20/28/285102

Influence of chain topology and bond potential on the glass transition of polymer chains simulated with the bond fluctuation model

J J Freire

Departamento de Ciencias y Técnicas Fisicoquímicas, Facultad de Ciencias, Universidad Nacional de Educación a Distancia (UNED), Senda del Rey 9, 28040 Madrid, Spain

E-mail: jfreire@invi.uned.es

Received 8 February 2008, in final form 21 April 2008
Published 2 June 2008
Online at stacks.iop.org/JPhysCM/20/285102

Abstract

The bond fluctuation model with a bond potential has been applied to investigation of the glass transition of linear chains and chains with a regular disposition of small branches. Cooling and subsequent heating curves are obtained for the chain energies and also for the mean acceptance probability of a bead jump. In order to mimic different trends to vitrification, a factor B gauging the strength of the bond potential with respect to the long-range potential (i.e. the intramolecular or intermolecular potential between indirectly bonded beads) has been introduced. (A higher value of B leads to a preference for the highest bond lengths and a higher total energy, implying a greater tendency to vitrify.) Different cases have been considered for linear chains: no long-range potential, no bond potential and several choices for B. Furthermore, two distinct values of B have been considered for alternate bonds in linear chains. In the case of the branched chains, mixed models with different values of B for bonds in the main chain and in the branches have also been investigated. The possible presence of ordering or crystallization has been characterized by calculating the collective light scattering function of the different samples after annealing at a convenient temperature below the onset of the abrupt change in the curves associated with a thermodynamic transition. It is concluded that ordering is inherited more efficiently in the systems with branched chains and also for higher values of B. The branched molecules with the highest B values in the main chain bonds exhibit two distinct transitions in the heating curves, which may be associated with two glass transitions. This behavior has been detected experimentally for chains with relatively long flexible branches.

1. Introduction

Vitrification is a process associated with fast cooling of liquids and mainly characterized by a loss of mobility which is not caused by a long-range organization of the molecules. In these conditions, the system becomes an amorphous solid or glass [1]. Vitrification does not correspond to a thermodynamic transition and, in fact, a glass is not in thermodynamic equilibrium. However, the process usually takes place in a narrow range of temperatures that permits the definition of an experimental glass transition temperature, T_g. The glass formation can be observed at slower cooling rates in some types of materials such as polymer melts [2], whose crystallization is partially or totally hindered.

The glass transition of polymer melts has been the object of several studies by numerical simulation in recent years [3–11]. Given the large timescales involved in the process and the need for considering a relatively large portion of the molecular systems, a substantial fraction of these studies have made use of simplified coarse-grained polymer models. Some of these studies have used the bond fluctuation model (BFM) [12, 13], devised to offer the computational benefit of lattices and the more realistic characterization of systems represented by the open space simulations. This

model offers a variety of bond lengths. Also, it permits the generation of successive configurations in a Monte Carlo (MC) simulation by means of a simple single bead jump. These features make this model adequate for the study of the statics and dynamics of vitrification when intramolecular and intermolecular interactions are included by means of adequate temperature-dependent potentials. A long-range potential that describes interactions between non-bonded close units is usually introduced to this purpose. However, the decrease of temperature also favors the system ordering or crystallization [3–6] if the mobility of the polymer units allows for the formation of long-range order. Vitrification takes place, however, in the amorphous parts of the system at an even lower temperature when mobility of the amorphous structure is severely limited.

Previous studies with the BFM have demonstrated that vitrification can only be investigated with the additional introduction of a bond-length potential [3, 6, 10]. This potential leads to a higher proportion of the longest bonds allowed in the model, which are able to trap some amount of empty space, reducing the system mobility and preventing the formation of ordered structures. In some of these studies, other intramolecular or intermolecular interactions are completely removed to avoid ordering [3] so that the temperature variation is only reflected in the bond potential effectiveness. A recent work on this issue has concluded that the bond potential should actually be much stronger than any long-range potential in order to mimic a realistic glass behavior [10]. This particular conclusion was achieved by using a fixed bond potential and several weakened forms of the long-range potential. Previous studies of the glass transition with the BFM have been focused on the study of linear chains.

In this work, we consider chains with a regular disposition of small branches (which we denote as 'branched chains') represented by the BFM in order to make a more systematic study of the possible of ordering in glass forming polymer melts. Most of our systems have a fixed long-range potential, which should consistently lead to the same range of temperatures for the possible thermodynamic transitions of the system, and differ in the strength of the bond potential and, also, in the polymer topology. Furthermore, we also include chains with different assignments of bond potentials within the chains (alternate bond potentials for linear chains, and different potentials in the main chain and branches in the case of nonlinear chains). Given the need to compare all these different cases, we have mainly restricted this work to a basic comparison of the cooling rates and also to the characterization of ordering or crystallization through the behavior of the collective scattering function in the simulation boxes. In particular, we investigate the possible increase of the collective scattering function of the simulation box at low q, due to the presence of inhomogeneities, and the sometimes associated appearance of Bragg peaks or an increase of their intensity for higher values of q.

2. Model and methods

The BFM [12, 13] offers a considerably higher number of empty positions available around an occupied site and, furthermore, it only needs a single and simple form of elementary move, particularly useful when it comes to writing codes applicable to nonlinear chains.

Table 1. $U(\mathbf{R})$ and $V(\mathbf{l})$ (from [6] and [14]). The vector coordinates are generic and valid for any specific combination of x, y or z.

Type of vector	$V(\mathbf{l})$	$U(\mathbf{R})$
$(\pm2, 0, 0)$	4.461	−3.177
$(\pm2, \pm1, 0)$	2.021	−2.275
$(\pm2, \pm1, \pm1)$	−0.504	−1.594
$(\pm2, \pm2, 0)$	Not allowed	−0.771
$(\pm3, 0, 0)$	−3.275	−0.319
$(\pm2, \pm2, \pm1)$	−3.478	−0.521
$(\pm3, \pm1, 0)$	−1.707	0

In the present work, the distance between adjacent lattice sites is adopted as the length unit and energies are given in k_BT units. We use a version of the model with an attractive–repulsive potential for bond energies, $V(\mathbf{l})$, depending on each particular bond vector, and a long-range potential $U(\mathbf{R})$, depending on the particular vector joining non-neighboring units (see table 1). Namely, we consider the potentials proposed by Wittkop *et al* [6] to mimic the 'glassy' behavior of polymer chains. Our version, however, introduces a numerical factor for the bond energy potential energy, B, with respect to the values employed by Wittkop *et al*, so that

$$V_B(\mathbf{l}) = BV(\mathbf{l}). \tag{1}$$

The consideration of factor B is inspired by recent results suggesting that the main features of the glass state can be only reproduced if the strength of the bond potential is somehow increased with respect to the long-range potential [10]. The present study, however, differs from the investigation performed in [10] in some substantial features. Firstly, a factor B is introduced here to increase the absolute values of the bond potential. Secondly, the temperatures T actually correspond to the factors, k_BT, that determine the Boltzmann weights associated with the potential energy terms, whose absolute values are presented in table 1. These two differences apparently mean that the temperature values in this work correspond to temperatures $(1 + B)^2$ times smaller than in [10], although this correspondence is not exact due to some differences in the specific forms of the potentials. We have considered several values of B. In particular, we have investigated the case $B = 0$ (no bond potential) and the range $B = 1$–5. We have also obtained some results without the long-range potential and $B = 1$.

Furthermore, our particular model considers linear chains and branched chains that are built by adding a single unit branch to every non-end bead in a linear chain. The main chain branching beads are treated as 'chiral atoms'. Consequently, we consider the plane formed by the two bonds in the main chain connected to every branching bead (when these two bonds are not in a collinear configuration) and define the side of this plane in which the first bead of the branch should remain along the simulation. The initial spatial disposition is assigned for each unit branch during the initial equilibration process. We have verified that substantial numbers of 'meso' and 'racemic' dyads are randomly generated by using this procedure.

The model includes the possibility of employing different values of B for different types of bonds. In particular, the case of different B factors on alternate bonds along a linear chain has been considered. This case can mimic some chains with a regular disposition of monomers (or larger groups of atoms) with different compositions and it may also apply to the description of some polymers with different side groups along the main chain structure. Also, we have performed simulations for our branched chains considering the cases of a different B factor (greater or smaller) for bonds in the branches with respect to the factor associated with bonds in the main chain.

In the present work, we have included n chains, each composed of N beads, in a cubic lattice of length L, with periodic boundary conditions [15]. Therefore, the simulations correspond to an NVT ensemble. The distance between adjacent sites, b, is taken as the length unit. Each one of the beads blocks the 26 lattice sites contained in the elementary cube centered at the bead site, which cannot be occupied by another bead to comply with the restrictions imposed for self-avoiding walk chains. This condition is totally equivalent to that established originally for the model [12, 13], in which each bead occupies a cube defined by eight lattice sites and a single lattice site cannot be simultaneously occupied by two beads. However, our procedure avoids the presence of a trivial form factor contribution of the unit cubes in the collective scattering factors. Bonds linking the beads may have lengths ranging between 2 and $\sqrt{10}$, but bond vectors of the type $(\pm 2, \pm 2, 0)$ are excluded to avoid bond crossing during the simulation. The value of L is chosen to be high enough that the number of interactions between different replicas of the same chain is very small, $L \geqslant 2\langle R^2\rangle^{1/2} + 5l$, where $\langle R^2\rangle$ is the mean quadratic end-to-end vector of a single self-avoiding walk chain and l is the root-mean squared bond distance in the absence of any type of numerical potentials ($l = 2.72$). In the present work, we have set $L = 84$ for all the cases. The number of chains is determined from the desired number of sites blocked by polymer beads, equivalent to the polymer volume fraction, $\Phi = 8\, nN\, L^{-3}$. This volume fraction is fixed to the value $\Phi = 0.5$, which gives a good representation of the melt state. Linear chains are constituted by $N = 40$ beads, while branched chains are composed of $N = 78$ beads; 40 of them form the main chain. Therefore, the non-end beads of the main chain define 38 branching points, which are connected with 38 single bead branches.

Initially, the chains form a packed configuration. Linear or branched chains are organized in successive arrays of extended conformations, placed as close as possible to avoid overlapping, i.e. at a distance of 2 for the linear chains. The separations between branched chains are 2 or 4 in the two different directions perpendicular to the main chain. The wider separation in a given direction allows for the location of the branch beads bonded to the main chain in this particular direction. All initial bond lengths are 2. These initial configurations are far from equilibrium but the simulation boxes contain a large empty space in contact with some of the chains, which eventually allows for a fast equilibration as has been previously verified for linear [15] and star [16] chains.

An equilibration run of 10^6 MC steps is performed to equilibrate the linear and branched chains without intermolecular or bond potentials, starting from their initial extended conformations. We have computed the mean quadratic radius of gyration in the last 2×10^5 steps, verifying that it is stable. Furthermore, we have compared its value, $\langle S^2\rangle = 78.5 \pm 0.5$, with the result obtained with a dilute (single chain) system at temperature $T = 4.67$, close to the θ state (same number of configurations), $\langle S^2\rangle = 82.5 \pm 0.5$. Both values are close, as is expected, since the chains are supposed to behave ideally in a melt and in the θ state. (A slight difference between both values is also found for linear chains, $\langle S^2\rangle = 61.6$ in the melt and $\langle S^2\rangle = 66.3$ at $T = 4.67$, as was reported in a previous study of conformational and dynamic properties with the same model [15].) These data confirm that our equilibration method (starting from extended conformations as described above) is also adequate for the apparently more difficult case of branched chains.

A second equilibration run, also of 1×10^6 steps, is performed at a conveniently high temperature ($T = 20$) for every system with a different set of potentials. Starting at this point, we perform cooling runs where the system temperature is gradually decreased. We have considered several cooling rates, corresponding to $\Delta T = -0.1$ per 5, 50, 500, 10^3, 5×10^3, 10^4 and 2.5×10^4 MC steps. The runs are finished when a very low temperature ($T = 0.1$ or 0.2) is reached. 'Isothermal annealing' processes are subsequently simulated at different low temperatures, using the configurations obtained from the cooling process. Most of these runs are of similar length to the equilibration processes, though sometimes they are significantly extended (up to 3×10^6 MC steps) in subsequent runs in order to try to detect the possible formation of inhomogeneities or ordered intermolecular structures. Furthermore, heating runs are also performed from the lowest temperature of the cooling processes, with the same rates as employed for cooling.

In order to detect intermolecular order, we have computed the collective scattering function of the systems. This function is obtained as

$$S_{\mathrm{coll}}(q) = 8n_{\mathrm{s}}^{-1}\left\langle \sum_{i}^{n_{\mathrm{s}}}\sum_{j}^{n_{\mathrm{s}}} f_i f_j \exp(\mathrm{i}\mathbf{q}\cdot\mathbf{R}_{ij})\right\rangle \qquad (2)$$

where the factor of eight takes into account that any of our beads actually represents eight unit sites in the original model. In equation (2), the average extends over a sample of different configurations (obtained at constant temperature), $\mathbf{q}$ is the scattering vector, depending on experimental settings, the vectors $\mathbf{R}_k(t)$ refer to the positions of the different $n_{\mathrm{s}} = L^3$ sites within the system and f_k is the contrast factor, related to the difference between the scattering factor due to the particular occupation of the site in a given configuration and the mean scattering factor of the system. Thus, for homopolymer systems

$$f_i = 1 - \Phi/8 \qquad (3a)$$

if site i contains a bead unit or

$$f_i = -\Phi/8 \qquad (3b)$$

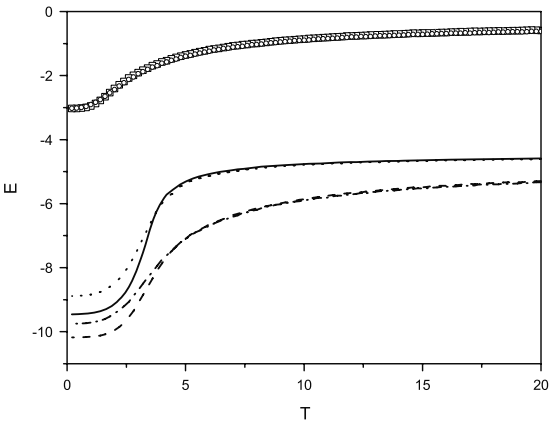

Figure 1. Cooling curves of the mean energy per bead for different systems. Cooling rate: $\Delta T = -0.1$ per 5×10^3 MC steps. Solid line, linear chain, $B = 0$; dashed line, linear chains, $B = 1$; dotted line, branched chains, $B = 0$; dash–dot line, branched chains, $B = 1$. Systems without a long-range potential, $B = 1$, are denoted by symbols. Squares, linear chains; circles, branched chains. Statistical uncertainties are always smaller than 0.02.

otherwise, in order to comply with the requirement that the global system, considered as a large single isotropic volume, does not scatter [15]. The practical range of values of $\mathbf{q}$ is limited by the periodic boundary condition in the simulation box:

$$q_k = (2\pi/L)n_k, \qquad k \equiv x, y, z, \quad n_k = 1, 2 \ldots, \qquad (4)$$

that also determines the smallest value of q. With these specifications, a homogeneous system should show small and isotropic values of $S_{\mathrm{coll}}(\mathbf{q})$ for the whole range of small and intermediate values of $\mathbf{q}$. (Error bars can be estimated from the standard deviations of the results corresponding to equivalent $\mathbf{q}$ vectors.) At large values of $\mathbf{q}$ local features of the model can be observed. If a thermodynamic transition occurs, however, $S_{\mathrm{coll}}(\mathbf{q})$ becomes large and anisotropic for small values of $\mathbf{q}$, due to the growing development of inhomogeneities, while Bragg peaks at high $\mathbf{q}$ demonstrate a long-range ordering associated with crystallization.

3. Results and discussion

In figure 1 we show the mean energy per bead, E, along cooling processes corresponding to six different cases. These curves have been obtained at a cooling rate of $\Delta T = -0.1$ per 5×10^3 MC steps. We consider linear and branched chains with bond potential, $B = 1$, or without this contribution ($B = 0$). We also include the results corresponding to systems without a long-range potential (linear or branched chains) but with bond potential ($B = 1$). All these curves exhibit a clear sigmoidal form, as has also been observed in previous simulations with the same model [6]. Considering only the systems with a long-range potential, the curves with $B = 1$ have lower energies than the curves with $B = 0$ since the bond potential gives a negative contribution to the energy. The curve corresponding to the linear chain without bond potential clearly shows the most abrupt transition. Comparing the curves with the same type of potential, the sharpest transitions always correspond to the linear chains. Although the form of the curves may indicate a first order transition, such as crystallization, the downwards curvature at high temperatures is a feature that can simply be associated with the asymptotic behavior of the energy at high temperatures. This behavior is implicit in the model. Thus, the sigmoidal shape is also observed in curves corresponding to the systems without long-range interactions, where segregation or ordering cannot occur since the change in temperature only affects the bond probabilities.

The explanation of the model-conditioned high temperature asymptote is simple. At very high temperatures, all the different chain configurations have similar statistical weights. Therefore, a further increase of temperature does not have any effect on the distribution of configurations and, consequently, the mean energy stays constant. The asymptotic regime is reached at higher temperatures when the total energy is greater and, consequently, the presence of a more negative contribution for the energetic bond potential implies a later arrival of the asymptotic behavior, though this behavior should eventually be reached anyway at conveniently high temperatures. Only simulations in the NPT ensemble [17] would be able to exhibit an increase in the number of vacancies in the system at higher temperatures, implying an increase of energy (decrease of favorable interactions) in this region. Although some algorithms have been designed to perform non-constant-volume simulations in lattices, these algorithms have not been implemented yet for the BFM.

However, the more abrupt curves exhibited by some of the curves obtained with long-range potential suggest a thermodynamic transition. This process is probably associated with ordering or crystallization in a part of the system. This seems to explain the differences between the curves corresponding to the linear and branched chains that share the same asymptotic limits at high temperature. One may also suspect that the thermodynamic transition explains the more marked sharpness in the curves of the models without a bond potential. In fact, the bond potential has been included in the bond fluctuation as an artifact to avoid ordering [3–6, 18]. It can be observed that the center of the sigmoidal transitions for all the curves corresponding to the systems with long-range potential in figure 1 is always placed at similar temperatures. In fact, these curves are sharp enough to give an estimate of a transition temperature, T_c. Their first derivatives provide the tentative value $T_c = 3.3 \pm 0.1$. However, it should be remarked that the onset of the thermodynamic transition can actually be assumed to occur at considerably higher values of T. However, this feature is more difficult to characterize since it is somewhat masked by the asymptotic bending of the curves. As expected, the systems without a long-range potential show an inflexion point at considerably lower temperature, which indicates a completely different physical behavior. Incidentally, the effect of branching is very small in these particular curves.

Since all curves shown in figure 1 are sigmoidal, the characterization of the glass transition in the low temperature region is not easy. This transition is generally marked by an abrupt change in the slope of the curves, associated with a discontinuity (not a peak) in the first derivative (specific heat).

Table 2. Estimation of the glass transition temperature for different systems and cooling rates.

System	T_g
Linear chains, $B = 0$	2.4 ± 0.2[a]
Branched chains, $B = 0$	2.0 ± 0.2[a]
Linear chains, $B = 1$	2.2 ± 0.2[a]
Branched chains, $B = 1$	1.8 ± 0.1[a]
Linear chains, $B = 1$, $U(\mathbf{R}) = 0$	1.1 ± 0.1[a]
Branched chains, $B = 1$, $U(\mathbf{R}) = 0$	1.0 ± 0.1[a]
Branched chains, $B = 1$	1.7 ± 0.1[b]
Branched chains, $B = 1$	1.5 ± 0.1[c]
Branched chains, $B = 1$	1.1 ± 0.1[d]
Linear chain, $B = 3$	3.5 ± 0.2[e]
Branched chains, $B = 3$	3.0 ± 0.2[e]
Branched chains, $B = 5$	4.5 ± 0.2[e]
Linear chains, alternate bonds[f]	3.2 ± 0.2[g]
Glassy branches[h]	3.3 ± 0.2[g]
Glassy main chain[i]	1.2 ± 0.1[g]

[a] Cooling rate: $\Delta T = -0.1$ per 5×10^3 MC steps.
[b] Cooling rate: $\Delta T = -0.1$ per 500 MC steps.
[c] Cooling rate: $\Delta T = -0.1$ per 50 MC steps.
[d] Cooling rate: $\Delta T = -0.1$ per 5 MC steps.
[e] All cooling rates.
[f] $B = 1$ or 5 for odd and even bonds.
[g] Cooling rate: $\Delta T = -0.1$ per 10^3 MC steps.
[h] $B = 5$ for bonds in the branches, $B = 1$ for bonds in the main chain.
[i] $B = 5$ for bonds in the main chain, $B = 1$ for bonds in the branches.

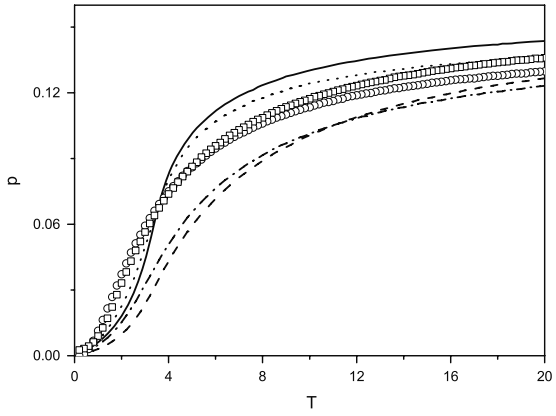

Figure 2. Cooling curves of the mean acceptance probability of a bead jump for different systems. Cooling rate: $\Delta T = -0.1$ per 5×10^3 MC steps. Solid line, linear chain, $B = 0$; dashed line, linear chains, $B = 1$; dotted line, branched chains, $B = 0$; dash–dot line, branched chains, $B = 1$. Systems without a long-range potential, $B = 1$, are denoted by symbols. Squares, linear chains; circles, branched chains. Statistical uncertainties are less than 2×10^{-4} for the highest temperatures and decrease to less than 10^{-5} for the lowest temperatures.

The curves in figure 1 suggest two regions at low temperature. In one of these regions, the value of the energy is practically constant (first derivative close to zero). The second region corresponds to a relatively narrow range of temperatures where the curve shows a constant slope. The intersection of the slopes corresponding to these two regions may be used as an estimate of the apparent glass transition temperatures (see table 2).

Rigidity is an important factor determining the glass transition temperature of many polymer systems [2]. In fact, in the comparison between real linear chains and chains with the same skeleton but with bulky side groups, the latter have a higher T_g because of the considerably higher rigidity of the main chain induced by the moiety. In order to investigate the rigidity due to branching in the present model we have calculated the mean quadratic distance between the end units of the backbone for the melt of branched chains without potential (infinite temperature). The result is $\langle R^2 \rangle = 460 \pm 2$ for the last 2×10^5 steps of the initial equilibration. This result can be compared with the slightly smaller value for the mean quadratic end-to-end distance of linear chains (same number of beads in the backbone) previously reported [15], $\langle R^2 \rangle = 370$. The conclusion is that the increase of rigidity due to branching is relatively small (a 12% increase in the characteristic ratio) and it should not be very relevant to determine the influence of topology on T_g. In fact, it is observed in table 2 that the branched chains show smaller values of the estimated T_g, in spite of their higher number of beads.

We have investigated whether similar conclusions can be achieved by making a representation of the mean acceptance probability for a bead jump, p, obtained with the cooling processes shown in figure 2. This average measures the possibility to perform the jump and, therefore, is related to the number of empty sites available around a bead and also to the Metropolis probability to perform a bead jump to these sites. These properties have been proposed or used to characterize local changes in the specific volume that are also indicative of a glass transition [6, 10, 11, 19–21]. We can actually observe some correlation in the features shown by the equivalent curves in figures 1 and 2, though the jump acceptance curves are markedly less sharp and have a common null value at low temperatures. In any case, our estimation of the glass transition temperature will be based on the energy curves, since these graphs provide a clearer distinction between the different cases, especially at low temperatures, where the acceptance ratios become very small.

In figure 2 it can also be observed that the acceptance ratios are higher for the linear chain than for the equivalent (same model) branched chains at high temperatures. Consequently, for a similar main chain length, the higher rigidity of the main chain in the branched chains seems to be the predominant factor to inherit bead jumps. However, the branched chains have considerably higher acceptance ratios in the low temperature range. In this case, the much higher number of chain ends with a higher mobility in the branched chains turns to be the mean factor. This effect is found in spite of the fact that the translational diffusion coefficients, D (obtained from representations of the mean squared global displacement of individual chains versus number of MC steps), are always considerably greater for the case of linear chains. For instance, comparing the systems with long-range potential and $B = 1$ at the intermediate temperature $T = 5$, the acceptance probability is larger for the branched chains, even though $D = 5 \times 10^{-6}$ for the linear chains and $D = 2 \times 10^{-6}$ for the branched chains at this temperature. Since the glass

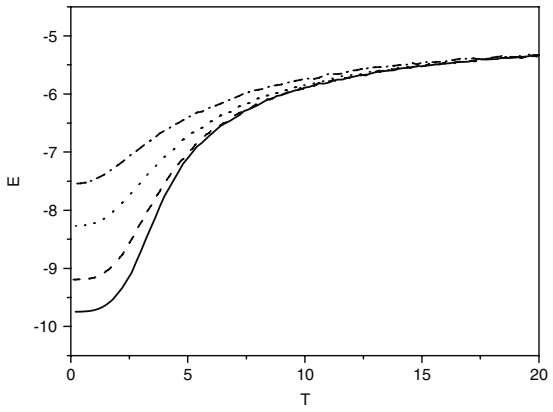

Figure 3. Cooling curves of the mean energy per bead corresponding to branched chains with $B = 1$ at different cooling rates. Solid line, $\Delta T = -0.1$ per 5×10^3 MC steps; dashed line, $\Delta T = -0.1$ per 500 MC steps; dotted line, $\Delta T = -0.1$ per 50 MC steps; dash–dot line, $\Delta T = -0.1$ per 5 MC steps. Statistical uncertainties are always smaller than 0.02.

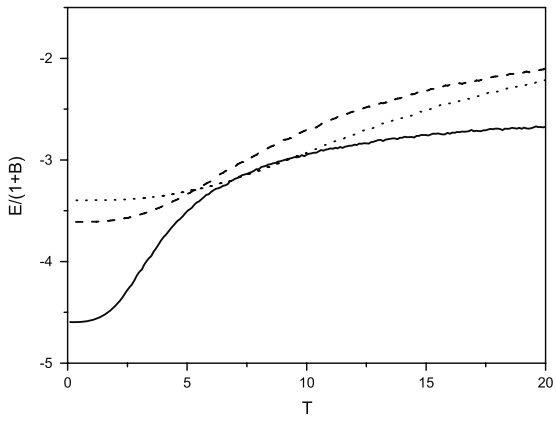

Figure 4. Cooling curves of the reduced mean energy per bead corresponding to branched chains with different values of B. Solid line, $B = 1$; dashed line, $B = 3$; dotted line, $B = 5$. Cooling rate: $\Delta T = -0.1$ per 10^3 MC steps. Statistical uncertainties are always smaller than 0.02.

transition occurs in the low range of temperatures, the mobility of end beads explains the lower T_g values exhibited by the branched chains. Actually, it has been experimentally verified for (similarly rigid) polyethylene chains of different degrees of branching that T_g decreases with a variable summing up the number of branching units and monomers in the branches [22].

In figure 3 we show the cooling curves of a branched chain with $B = 1$ obtained with different cooling rates ($\Delta T = -0.1$ per 5, 50, 500 and 5×10^3 MC steps). All these curves show similar sigmoidal trends. Faster cooling processes are obviously associated with less abrupt overall transitions. The first derivatives show broader peaks for the curves corresponding to the faster cooling processes which complicate the characterization of a transition temperature. However, all these peaks are compatible with our estimate, $T_c \cong 3.3$. Assuming that the glass transition can be characterized by the point where the slopes corresponding to the two linear regions at low temperature intercept, we can observe that the fastest rate curves correlate with the lowest glass transitions (see table 2). This tendency may be justified by considering that the T_g estimates are strongly biased by a thermodynamic process occurring at higher temperatures. It can be conjectured that the slowest cooling processes may contain larger crystalline regions acting as effective crosslinks. Therefore, the amorphous parts of the system have less mobility, increasing the glass transition temperature.

In figure 4, we show the results obtained for the branched chain with different values of B for the cooling rate of $T = -0.1$ per 10^3 MC steps. In order to compare more easily the different curves, the energy values are divided by the factor $(1 + B)$. It can be clearly observed that higher values of B tend to retard the asymptotic regime. As a consequence, the glass transition temperature is increased and becomes closer to the possible transition temperature. Therefore, the sigmoidal shape of the curves can effectively be inhibited or even eliminated by increasing B. From this point of view, the value $B = 5$ could be adequate to give a particularly good description of the glass transition.

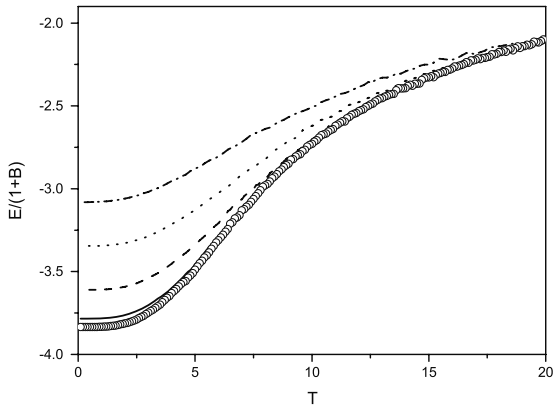

Figure 5. Cooling curves of the reduced mean energy per bead corresponding to branched chains with $B = 3$ at different cooling rates. Circles, $\Delta T = -0.1$ per 2.5×10^4 MC steps; solid line, $\Delta T = -0.1$ per 10^4 MC steps; dashed line, $\Delta T = -0.1$ per 10^3 MC steps; dotted line, $\Delta T = -0.1$ per 50 MC steps; dash–dot line, $\Delta T = -0.1$ per 5 MC steps. Statistical uncertainties are always smaller than 0.02.

The estimation of the glass transition from these three curves is also given in table 2. The result for $B = 5$ is close to our estimation of $T_c \cong 3.3$ for $B = 0$ or 1. A useful model should be able to provide ratios between crystallization and the glass temperatures following the main trend of most real polymers, for which vitrification occurs at temperatures significantly lower than possible crystallization. Otherwise, crystallization is not possible from the kinetic point of view, as actually happens in the case of our model with $B = 5$. Therefore, our choice $B = 3$ is more descriptive of these realistic polymer systems. Even though the curve for $B = 3$ shows a sigmoidal shape at high temperatures, the slope is constant in the range of temperatures for which ordering could occur.

In figure 5 we show the results for a branched chain with $B = 3$ obtained at different cooling rates ($\Delta T = -0.1$ per 5, 50, 10^3, 10^4 and 2.5×10^4 MC steps). It can be observed that

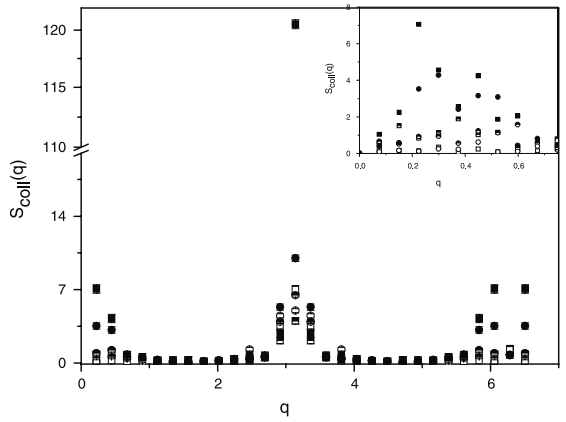

Figure 6. Collective scattering function, $S_{\rm coll}\,(q)$, for different systems at the lowest temperatures of the cooling process. Filled squares, linear chain, $B = 0$; filled circles, branched chains, $B = 0$; half-filled squares, linear chains, $B = 1$; half-filled circles, branched chains, $B = 1$; open squares, linear chains, $B = 3$; open circles, branched chains, $B = 3$. Inset: low q detail.

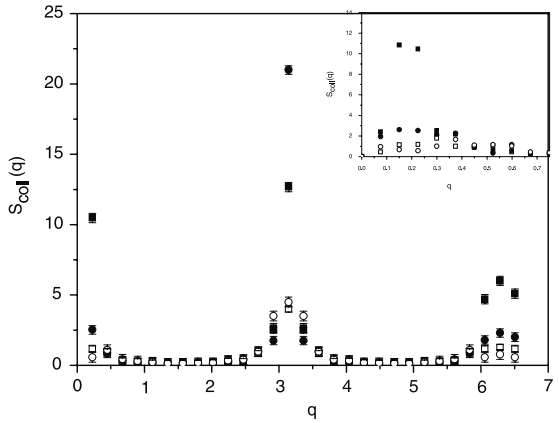

Figure 7. Collective scattering function, $S_{\rm coll}\,(q)$, at $T = 3.7$, for linear and branched chains with $B = 1$, after annealing with different MC steps. Open squares, linear chains, 10^5 MC steps; open circles, branched chains, 10^5 MC steps; filled squares, linear chains, 10^6 MC steps; filled circles, branched chains, 10^6 MC steps. Inset: low q detail.

the estimate of $T_{\rm g}$ from these curves is practically constant. The results for $B = 5$ at different cooling rates yield similar conclusions. Therefore, the marked influence of the sigmoidal shape of the curves in the estimation of $T_{\rm g}$ observed for the $B = 1$ results is eliminated when B is increased, which can be considered as an indirect verification of the absence of a significant thermodynamic transition in the $B > 1$ systems.

A more direct proof of the inhibition of any possible crystallization process for higher values of B can be made by computing the scattering function, $S_{\rm coll}(q)$. This function has been previously used to investigate the local structure (large q values) and the isothermal compressibility (low q range) in the melt and glass state for polymer systems without long-range potential [4, 13]. The collective scattering function for athermal polymer systems exhibits a flat form close to the value $S_{\rm coll}(q) \cong 0.2$ at low q [13, 23]. In our case, we are interested to characterize the possible presence of crystallization in the investigated systems. The onset of this feature should induce the appearance of Bragg peaks due to long-range ordering. Moreover, the formation of a denser phase may be marked by growing inhomogeneities, eventually leading to a divergence at $q \to 0$ when the ordered parts of the system become of substantial size. In figure 6, we present the curves corresponding to results for different systems obtained at the lowest temperature of the cooling process ($T = 0.2$). A very prominent first Bragg peak is observed for the system of linear chains with $B = 0$. This peak corresponds to the closest allowed distance, 2, between beads, $q \cong \pi$. The rest of the systems show a lower first Bragg peak that may simply be indicative of a liquid structure [13]. However, both the linear chain and branched chain systems with $B = 0$ clearly show a peak at low q and marked second Bragg peaks. Incidentally, the trivial peak at $q = 2\pi$ due to the contribution of the unit cubes in the original BFM description should not appear with the present model, that only considers a single unit per bead. Therefore, all these systems exhibit some indication of ordering and inhomogeneities, though the much smaller intensity of the first Bragg peak observed for the branched chains reveals a considerable inhibition of crystallization. In spite of some statistical noise, a closer inspection of the results at low q (inset in figure 6) clearly indicates the presence of smaller inhomogeneities even for the $B = 1$ systems for linear and branched chains. Consequently, all the systems with B smaller than 3 seem to undergo some kind of thermodynamic transition, in agreement with the conclusions obtained from the energy and acceptance probability curves.

The features marking a phase transition should progressively be enhanced in an annealing process at a temperature lower than the onset of the crystallization process but higher than the glass transition temperature, where the ordered regions are able to grow at an adequate rate. In figure 7, we show results obtained for the model with $B = 1$ (linear and branched chain) with an annealing at $T = 3.7$, value close to the estimated temperature for the center of the possible transitions in the systems showing a sigmoidal shape. We observe a clear increase in the intensity of the Bragg peaks and at low values of q. This is correlated with the progressive displacement of the low q peak for the linear chains as annealing progresses, observed in the inset of figure 7. The changes observed for the second Bragg peak and at low q are less dramatic for the branched chains (the intensities in the first Bragg peak are similar for both linear and branched chains, though the branched chain is thinner) confirming the important inhibition of inhomogeneities in these systems. However, ordered structures are apparently formed even for this type of chain, unless B is greater than unity.

Inhomogeneities and ordering could also appear in other systems if a long annealing is performed. For higher values of B, we have mainly focused our investigation on the possible presence of inhomogeneities for linear chains, since, according to the above discussion, these chains show a larger tendency to have a thermodynamic transition. In figure 8, we observe that the intensities are remarkably small at low q for $B = 3$. Peaks are considerably lower and close to the statistical errors in this

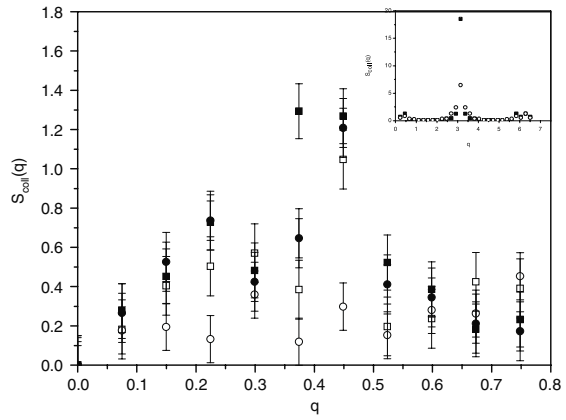

Figure 8. Collective scattering function, $S_{\rm coll}\ (q)$, for low q at $T = 3.7$, for linear chains with $B = 3$, after annealing with several different MC steps. Open circles, 10^5 MC steps; open squares, 10^6 MC steps; filled circles, 2×10^6 MC steps; filled squares, 3×10^6 MC steps. Inset: wider q range.

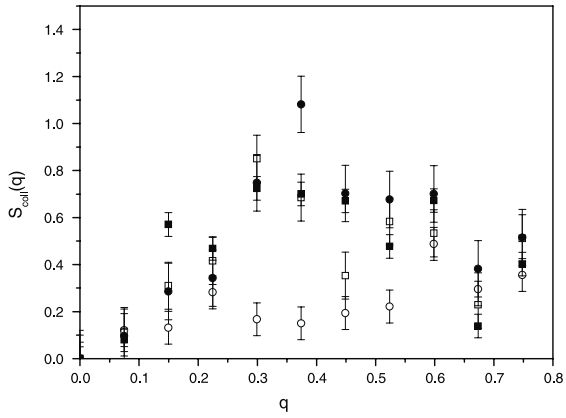

Figure 9. Collective scattering function, $S_{\rm coll}\ (q)$, for low q at $T = 3.7$, for linear chains with alternate bonds of $B = 1$ and 5, after annealing with several different MC steps. Open circles, 10^5 MC steps; open squares, 10^6 MC steps; filled circles, 2×10^6 MC steps; filled squares, 3×10^6 MC steps.

q region. The system shows a slight long-range inhomogeneity growth at the earlier steps of the annealing, but the rate of this effect is retarded and is practically stopped at longer times. In the inset of figure 8, we can verify that Bragg peaks in the linear chains remain practically constant during annealing (the intensity of the first peak is similar for the short and long annealing, though the peak is thinner in the latter case; the second peak is remarkably small in both systems). An even clearer inhibition in the ordering growth is found for a model of a linear chain having the alternate values of $B = 1$ or $B = 5$ for odd and even bonds along the chain skeleton. With this choice we try to mimic the presence of bulky (prone to vitrify) monomers in the polymer structures. The model shows remarkably small and close to constant values of the scattering function for small values of q after a moderate number of annealing steps; see figure 9.

In figure 10, we present the cooling curves of $\Delta T = -0.1$ per 10^3 MC steps corresponding to different types of chains,

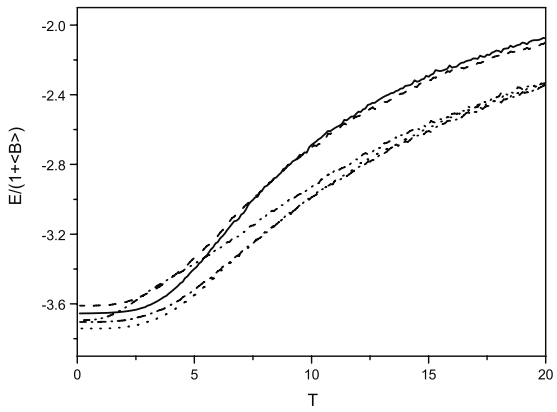

Figure 10. Cooling curves of the reduced mean energy per bead corresponding to different systems with $\langle B\rangle \cong 3$. Solid line, linear chains, $B = 3$; dashed line, branched chains, $B = 3$; dotted line, linear chains with alternate bonds of different B, $B = 1$ and 5; dash–dot line, branched chains with $B = 1$ for the main chain bonds and $B = 5$ for the branch bonds; dash–dot–dot line, branched chains with $B = 5$ for the main chain bonds and $B = 1$ for the branch bonds. Cooling rate: $\Delta T = -0.1$ per 10^3 MC steps. Statistical uncertainties are always smaller than 0.02.

all of them with a mean value of B close to 3. Comparing the curves for a linear and a branched chain, both of them for $B = 3$, it is observed that the linear chain exhibits a slightly sharper overall transition. The estimated value of $T_{\rm g}$ for the linear chain is higher ($T_{\rm g} \cong 3.5$) than for the branched structure. We include in figure 10 the cooling curve for the linear chain mixing alternate $B = 1$ and 5 bonds. This curve exhibits a considerably large region with constant slope above $T_{\rm g}$ so that sigmoidal shape is only observed when high temperatures ($T > 10$) are considered. This is consistent with the strong inhibition of ordering shown by the scattering curves. Its glass transition is estimated to be slightly smaller than the result for linear chains with a single $B = 3$ value (table 2).

Also, we include cooling curves that correspond to mixed models of branched chains where either the main chain or the branch bonds have more tendency to form a glass, $B = 5$, while we assign $B = 1$ to the other chain bonds. The curve corresponding to more rigid, or 'glassy', units in the branches is similar to that corresponding to linear chains with alternate B values. However, the chains with a 'glassy' main chain are substantially different, with a broader linear region above $T_{\rm g}$, as can be observed in figure 10. This region extends up to remarkably high temperatures. Moreover, the apparent glass transition at very small temperatures, $T_{\rm g} \cong 1.2$, is close to the smaller $T_{\rm g}$ values obtained for $B = 1$ with higher cooling rates (which supposedly may inhibit the effect of the previous abrupt thermodynamic transition on the determination of $T_{\rm g}$ for this value of B) or in the absence of a long-range potential.

We have obtained heating curves with the same rates for the T variation used for cooling. Heating starts at the lowest T reached in the cooling process without annealing. The results for the mixed model of a flexible main chain and rigid, or 'glassy', branches are shown in figure 11. There is some hysteresis above $T_{\rm g}$, but both curves converge to a

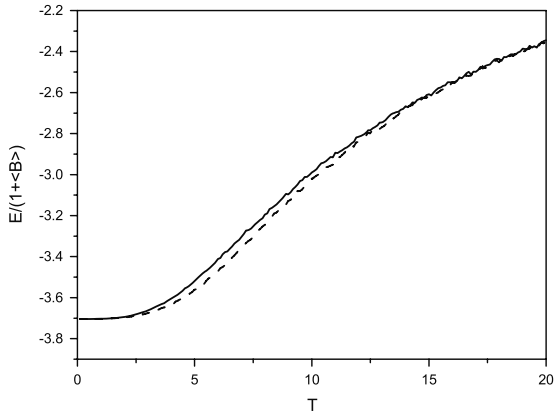

Figure 11. Cooling (solid line) and heating (dashed line) curves of the reduced mean energy per bead corresponding to branched chains with $B = 1$ for the main chain bonds and $B = 5$ for the branch bonds. Rates: $|\Delta T| = -0.1$ per 10^3 MC steps. Statistical uncertainties are always smaller than 0.02.

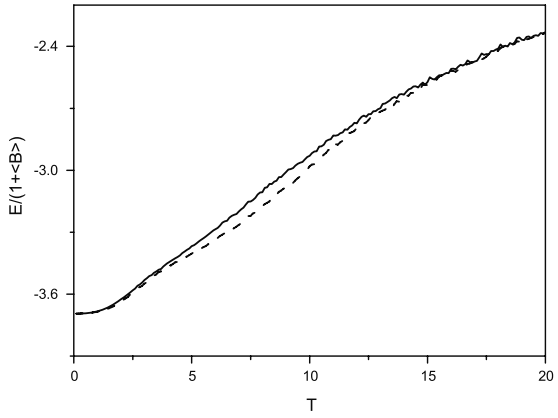

Figure 12. Cooling (solid line) and heating (dashed line) curves of the reduced mean energy per bead corresponding to branched chains with $B = 5$ for the main chain bonds and $B = 1$ for the branch bonds. Rates: $|\Delta T| = -0.1$ per 10^3 MC steps. Statistical uncertainties are always smaller than 0.02.

common equilibrium asymptotic behavior at large values of T. A similar description applies to the rest of the investigated systems except for the mixed model of a rigid or 'glassy' main chain with more flexible branches. The cooling and heating curves for this particular system are shown in figure 12. The lower heating curve shows two clearly different regions above T_g. The first region, between T_g and T_t, is similar to the curves observed in other systems, with a slight hysteresis. However, at temperatures above $T_t \cong 5$, the heating curve bends downwards and the hysteresis is significantly increased. Since our estimates for T_g and T_t roughly correspond to the glass transition temperatures of homogeneous chains with $B = 1$ and 5 bonds, respectively, the conclusion is that these systems show local heterogeneity, with two regions of independent glass transitions.

Real polymers that may correspond to this model are chains with bulky main chain monomers and flexible branches. In particular, these simulation results seem to be consistent with dielectric relaxation [24] and NMR [25] experiments performed for poly(di-n-alkylitaconates), which apparently exhibit two glass transitions. Earlier investigations with poly(mono-n-alkylitaconates) [26] reported abnormal curvatures or endothermic peaks in DSC thermograms that were tentatively assigned to side chain crystallization.

In summary, we have confirmed the usefulness of employing stronger bond potentials to provide a better description of the glass transition in models that include a long-range potential. Compared with the linear chain systems, branched chains show a clear inhibition of inhomogeneities and possible ordering and they show slightly smaller glass transition temperatures. The use of two different sets of bond potentials within a given type of chain is useful to describe more complex systems, as in the case of branched chains with a rigid main chain and flexible branches, for which two different glass transitions have been experimentally detected.

Acknowledgments

This work was supported by project CTQ2006-06446 from DGI-MEC Spain. The author thanks Professor Arturo Horta (Universidad Nacional de Educación a Distancia, Spain) and Professor José Luis Gómez Ribelles (Universidad Politécnica de Valencia, Spain) for useful discussion and also Dr. Carl McBride (Instituto de Química Física Rocasolano, CSIC, Spain) for revising the manuscript.

References

[1] Zallen R 1983 *The Physics of Amorphous Solids* (New York: Wiley)
[2] Cowie J M G 1973 *Polymers: Chemistry and Physics of Modern Materials* (London: Chapman and Hall)
[3] Baschnagel J, Binder K and Wittmann H-P 1993 *J. Phys.: Condens. Matter* **5** 1597
[4] Baschnagel J and Binder K 1994 *Physica* A **204** 47
[5] Baschnagel J 1996 *J. Phys.: Condens. Matter* **8** 9599
[6] Wittkop M, Hölzl T, Kreitmeier S and Göritz D 1996 *J. Non-Cryst. Solids* **201** 199
[7] Hölzl T, Wittkop M, Kreitmeier S, Trautenberg H L and Göritz D 1997 *J. Chem. Soc. Faraday Trans.* **93** 2185
[8] Binder K, Baschnagel J, Bennemann C and Paul W 1999 *J. Phys.: Condens. Matter* **11** A47
[9] Bennemann C, Paul W, Baschnagel J and Binder K 1999 *J. Phys.: Condens. Matter* **11** 2179
[10] Molina-Mateo J, Meseguer-Dueñas J M and Gómez-Ribelles J L 2005 *Polymer* **46** 7463
[11] Molina-Mateo J, Meseguer-Dueñas J M and Gómez-Ribelles J L 2006 *Macromol. Theory Simul.* **15** 32
[12] Carmesin I and Kremer K 1988 *Macromolecules* **21** 2819
[13] Paul W and Baschnagel J 1995 *Monte Carlo and Molecular Dynamics Simulations in Polymer Science* ed K Binder (New York: Oxford University Press)
[14] Grassberger P 1997 *Phys. Rev.* E **56** 3682
[15] Rubio A M, Lodge J F M, Storey M and Freire J J 2002 *Macromol. Theory Simul.* **11** 171
[16] Di Cecca A and Freire J J 2002 *Macromolecules* **35** 2851
[17] Frenkel D and Smit B 1996 *Understanding Molecular Simulation* (San Diego, CA: Academic)
[18] Wittkop M, Kreitmeier S and Göritz D 1996 *J. Chem. Phys.* **104** 3373
[19] Vollmayr-Lee K 2001 *J. Chem. Phys.* **121** 4781

[20] Wittmann H-P, Kremer K and Binder K 1992 *J. Chem. Phys.* **96** 6291
[21] Lawlor A, Reagan D, McCullagh G D, de Gregorio P, Tartaglia P and Dawson K A 2002 *Phys. Rev. Lett.* **89** 245503
[22] Mäder D, Heinemann J, Walter P and Mülhaupt R 2000 *Macromolecules* **33** 1254
[23] Rubio A M, Lodge J F M and Freire J J 2002 *Macromolecules* **35** 5295
[24] Arrighi V, McEwen I J and Holmes P F 2004 *Macromolecules* **37** 6210
[25] Genix A-C and Lauprêtre F 2006 *J. Non-Cryst. Solids* **352** 5035
[26] Diaz-Calleja R, Ribes-Greus A, Gargallo L and Radić D 1991 *Polym. Int.* **25** 51